Proc. Natl. Acad. Sci. USA
Vol. 93, pp. 5067–5071, May 1996
Neurobiology

Spatial localization of calcium channels in giant fiber lobe neurons of the squid (*Loligo opalescens*)

MATTHEW B. MCFARLANE* AND WILLIAM F. GILLY†

Departments of *Molecular & Cellular Physiology and †Biological Sciences, Hopkins Marine Station of Stanford University, Pacific Grove, CA 93950

Communicated by R. Llinás, New York University Medical Center, New York, NY, September 25, 1995

ABSTRACT **Whole-cell voltage clamp was used to investigate the properties and spatial distribution of fast-deactivating (FD) Ca channels in squid giant fiber lobe (GFL) neurons. Squid FD Ca channels are reversibly blocked by the spider toxin ω-Agatoxin IVA with an IC_{50} of 240–420 nM with no effect on the kinetics of Ca channel gating. Channels with very similar properties are expressed in both somatic and axonal domains of cultured GFL neurons, but FD Ca channel conductance density is higher in axonal bulbs than in cell bodies at all times in culture. Channels presumably synthesized during culture are preferentially expressed in the growing bulbs, but bulbar Ca conductance density remains constant while Na conductance density increases, suggesting that processes determining the densities of Ca and Na channels in this extrasomatic domain are largely independent. These observations suggest that growing axonal bulbs in cultured GFL neurons are not composed entirely of "axonal" membranes because FD Ca channels are absent from the giant axon *in situ* but, rather, suggest a potential role for FD Ca channels in mediating neurotransmitter release at the motor terminals of the giant axon.**

All excitable cells express voltage-dependent Ca channels, and proper spatial localization of Ca channels in the plasma membrane of neurons is required for cellular function (1). Although most studies have been carried out on neuronal cell bodies (2, 3), some have focused on isolated nerve terminal preparations, where Ca channels in the presynaptic element provide the Ca influx that triggers neurotransmitter release (4, 5). In general, these Ca channels inactivate very little during a maintained depolarization and close (deactivate) very quickly after repolarization. Rapid efficient signaling is provided by the close proximity of these Ca channels to vesicle fusion and release sites (5–7), but very little is known about the mechanisms involved in establishing and maintaining such a specialized spatial distribution.

Ca channels have been extensively studied in the presynaptic terminal of the squid giant synapse (5, 8, 9), but these channels are synthesized in the soma of a giant interneuron in the brain that is not particularly amenable to experimental study. The postsynaptic element of this synapse is the giant motor axon, formed by fusion of small axons of several hundred giant fiber lobe (GFL) neurons in the stellate ganglion (10). This neuron offers an alternative system for studying Ca channel biophysics and localization. Dissociated GFL neurons in culture often retain a portion of the initial unfused axon segment that displays distal growth of a neuroma-like bulb. Intrinsic polarity is maintained in these neurons, as evidenced by a high density of tetrodotoxin-sensitive Na channels in the growing axonal bulb and their absence in the cell body (11). Although previous studies on cell bodies of cultured GFL neurons lacking axonal bulbs have revealed fast-deactivating (FD) Ca channels (12) that are blocked by cadmium ions (13, 14), neither the pharmacological sensitivity to more specific toxin blockers nor the pattern of spatial distribution has been addressed.

In this study we demonstrate that ω-Agatoxin-IVA (ω-Aga-IVA) sensitive FD Ca channels are present in the axonal bulbs of cultured GFL neurons, and, like Na channels, are maintained there at a higher density than in cell bodies. Although both bulbar surface area and Na channel density increase over time in culture, Ca channel densities in both bulbs and somata remain relatively constant. Mechanisms for regulating Na and Ca channel expression in the same extrasomatic domain thus appear to be quite different. FD Ca channels exhibit a pharmacological profile similar to Ca channels at the squid giant synapse (9, 15) and show biophysical properties comparable to many presynaptic Ca currents measured *in situ* (5, 16, 17). Given that native giant axons are essentially devoid of FD Ca channels (18), these observations suggest that FD Ca channels may be normally expressed in the motor terminals of the giant axon and that both axonal and motor terminal components are incorporated into axonal bulbs *in vitro*.

METHODS

Cell Isolation and Culture. GFL neurons were isolated from stellate ganglia of adult *Loligo opalescens* and cultured at 16–17°C in a medium (L-15, GIBCO) supplemented with 263 mM NaCl, 4.6 mM KCl, 49.5 mM $MgCl_2$, 2 mM Hepes, 2 mM L-glutamine, penicillin G (50 units/ml), and streptomycin (0.5 mg/ml) (11). Either 4.5 or 9.1 mM $CaCl_2$ was also added to the medium with no observable differences in phenomena reported in this paper.

Whole-Cell Recording. Whole-cell voltage clamp was performed using pipettes (0.5–1.0 MΩ) filled with one of two internal solutions with no observable differences in Ca currents. The first contained 375 mM tetramethylammonium (TMA) glutamate, 59 mM TMA-OH, 25 mM TMA-F, 17 mM TMA-Cl, 17 mM tetraethylammonium (TEA) EGTA, 5 mM CsCl, 8.3 mM Hepes, and 4 mM Mg ATP. In several experiments CsCl was omitted. No effects of internal fluoride on the basic properties of the Ca current (I_{Ca}) described in conjunction with Figs. 1 and 2 were found in experiments using this internal solution in which TMA-F was replaced with TMA-Cl and, 1 mM $CaCl_2$ and 10 mM TEA-EGTA were included. The second internal solution contained 350 mM *N*-methyl-D-glucamine (NMG) gluconate, 50 mM TMA-F, 25 mM TEA-Cl, 100 mM sodium gluconate, 5 mM TMA-EGTA, 10 mM Hepes, and 4 mM MgATP. No significant differences in I_{Ca} were observed between these two solutions. The standard external solution contained 480 mM NaCl, 50 mM $CaCl_2$, 10 mM $MgCl_2$, 5 mM CsCl, 10 mM Hepes, and 500 nM tetrodotoxin. In some cases external Na was fully replaced with NMG. All solutions were adjusted to 1000 milliosmolar and pH 7.8. ω-Aga IVA (Bachem, provided by Pfizer) solutions were

The publication costs of this article were defrayed in part by page charge payment. This article must therefore be hereby marked "*advertisement*" in accordance with 18 U.S.C. §1734 solely to indicate this fact.

Abbreviations: GFL, giant fiber lobe; FD, fast deactivating; SD, slowly deactivating; ω-Aga IVA, ω-Agatoxin IVA; *I*, current; *V*, voltage; *g*, conductance; *G*, conductance density.

freshly prepared from a stock solution, and test and control solutions contained lysozyme at 0.1 mg/ml.

Currents were recorded with a conventional patch-clamp amplifier with series resistance (R_s) and capacitance compensation and were filtered at 10 kHz with an 8-pole Bessel filter and sampled at 2–100 kHz. Linear ionic and capacity currents were subtracted using a P/−4 method from the holding potential of −80 mV. Selective measurement of "whole-cell" I_{Ca} from somatic and axonal bulb domains was made possible by cutting the connecting axon with a sharpened tungsten microelectrode (11). Experiments were performed at 10–15°C.

Data Analysis. Specific Ca conductance density through FD Ca channels (G_{FD}, in nS/pF) was estimated as follows. (*i*) An effective reversal potential (V_{Ca}) was estimated from a plot of peak I_{Ca} versus pipette voltage (V) as indicated in Fig. 1*C*. (*ii*) Tail currents were recorded at −80 or −120 mV after test pulses of varying amplitude, and the slowly deactivating (SD) component of each record was fit with a single exponential (τ_{SD} = 1.2–1.5 ms at −80 mV). These fits were then subtracted from the parent records (see Fig. 2 *A* and *B*). (*iii*) Peak amplitude of the residual FD Ca tail current (I_{FD}; τ = 150–200 μs at −80 mV) was measured for each activating voltage, and this value was used to calculate conductance, g_{FD}, achieved at the test pulse voltage as $g_{FD} = I_{FD}/(V - V_{Ca})$, where V is the pipette voltage during the tail current. (*iv*) G_{FD} was obtained by dividing g_{FD} by cell input capacitance, measured by integration of the transient current generated by a −10 mV step. Effective R_S values (14) for these measurements were low in both axotomized somata (0.38 ± 0.04 MΩ) and axonal bulbs (0.62 ± 0.04 MΩ), and errors in voltage control at the peak of tail currents were <5 mV and have been ignored.

For some "pairs" (see Table 1) of axotomized somata and axonal bulbs, this complete analysis was not possible, because the large size of some somata sometimes resulted in slow tail currents that compromised tail amplitude measurement. In these cases, I_{FD} was estimated from peak I_{Ca} flowing during the test pulse by multiplying I_{Ca} by the appropriate mean fraction of FD I_{Ca} in axonal bulbs (0.822 ± 0.010, n = 33) or axotomized somata (0.624 ± 0.040, n = 11), with $g_{FD} = I_{Ca}/(V - V_{Ca})$, where V is the test pulse voltage. Errors in voltage control in these measurements were also <5 mV. All data are expressed as the means ± SEM.

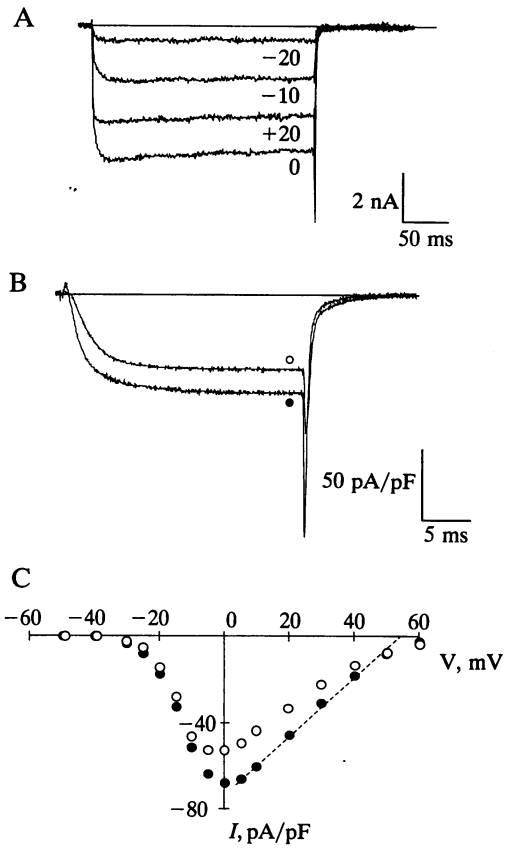

FIG. 1. Whole-cell I_{Ca} of squid GFL neurons. (*A*) I_{Ca} obtained by step depolarization to the indicated voltages from a holding potential of −80 mV for 250 ms. Currents were recorded from an axonal bulb after 3 days in culture (axonal bulb 4, R_S = 0.81 MΩ and C_{in} = 12.2 pF) where R_S is the series resistance and C_{in} is input capacitance. (*B*) I_{Ca} density at 0 mV in the axonal bulb (solid circle) and axotomized soma (open circle) of a day 7 GFL neuron obtained by dividing I_{Ca} by input capacitance (axonal bulb 31, R_S = 0.68 MΩ and C_{in} = 27.4 pF; axotomized soma 24, R_S = 0.67 MΩ and C_{in} = 82.9 pF). (*C*) Peak (25-ms step duration) I_{Ca} density–V relations for the axonal bulb (solid circles) and axotomized soma (open circles) of *B*. V_{Ca} is estimated from the linear fit of the rising phase of the I_{Ca} density–voltage curve for the axonal bulb (52.6 mV).

RESULTS

Whole-Cell I_{Ca} of GFL Neurons. GFL neurons show very little inactivation of I_{Ca} (Fig. 1*A*), and there is no apparent relationship among the degree or rate of inactivation and the site of channel expression (i.e., soma or axonal bulb), the amount of time cells are cultured, or the Ca buffering strength of the internal solution [comparison with a fluoride-free internal solution with intracellular Ca concentration estimated to be 100 nM (19), data not illustrated]. I_{Ca} in GFL neurons is thus essentially "noninactivating," and in this regard, resembles that in the squid presynaptic terminal (5), chicken parasympathetic nerve terminals (16), and *Xenopus* motoneuron terminals (17).

Properties of I_{Ca} are very similar in the cell body and axonal bulb of an individual GFL neuron (Fig. 1*B*), but a higher I_{Ca} density in the axonal bulb was observed in every GFL cell where recording from both domains was achieved (n = 24; see also below). Peak I_{Ca} density is plotted as a function of V for this bulb (solid circles) and soma (open circles) in Fig. 1*C*, and such similarity of these I_{Ca}–V relations was observed in every pair-wise comparison.

A complete analysis of the properties of I_{Ca} in each spatial domain is complicated by the apparent presence of two Ca channel types that are most reliably distinguished from one another by their deactivation kinetics (12). SD channels close 8–10 times more slowly than FD Ca channels, resulting in biexponential tail currents. Under these conditions, SD Ca channels underlie a minor portion of total I_{Ca}, and have generally been ignored (13), but in the present study, we specifically estimated the amount of FD Ca conductance by analyzing tail currents. Fig. 2*A* shows tail currents at −80 mV from the axonal bulb (solid trace) and axotomized soma (dotted trace) of a GFL neuron after a 25-ms step to +60 mV along with the least-squares fits of a single exponential to the SD portion of each trace.

Subtraction of each fit from the respective total tail current yields the FD Ca tails illustrated in Fig. 2*B*. This analysis reveals that axonal bulbs have a higher percentage of FD Ca current than do axotomized somata [82 ± 1% (n = 33) of total vs. 62 ± 4% (n = 11), respectively] and that axonal bulbs also have a greater FD Ca current density (see below). FD Ca channels may deactivate at a slightly faster rate in axonal bulbs (Fig. 2*B*), but the difference is small. Peak amplitude of the residual FD tail current is used to calculate G_{FD}, and G_{FD} is plotted as a function of activation voltage in Fig. 2*C*. To determine maximal G_{FD}, G_{FD}–V relations were fit with a single Boltzmann function. Aside from G_{max}, which is obviously larger for axonal bulbs, the fit parameters of axonal bulbs and somata are very similar.

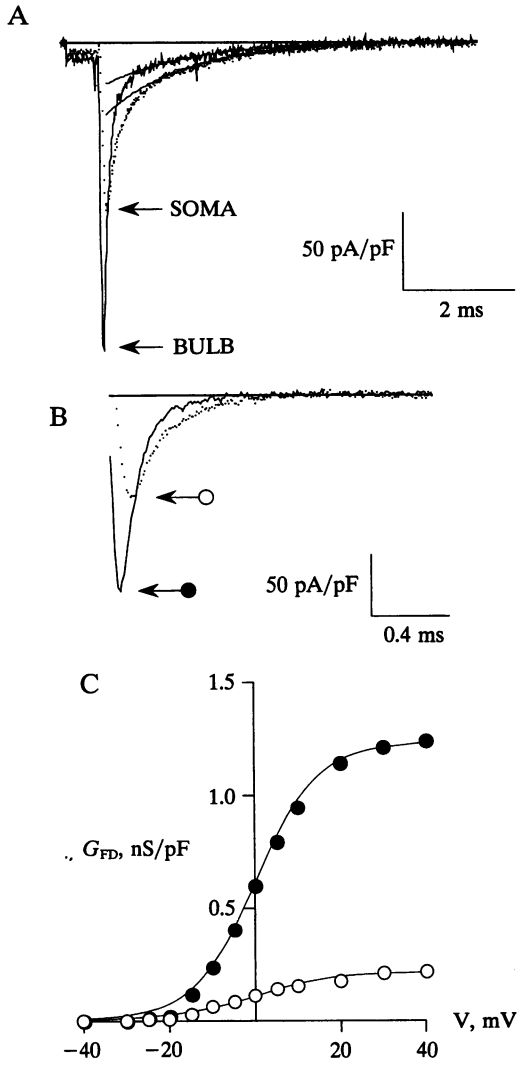

FIG. 2. Properties of I_{Ca} tails in axonal bulbs and axotomized somata. (*A*) Tail currents obtained at −120 mV after a test pulse to +60 mV for 10 ms from the axonal bulb (solid trace) and axotomized soma (dotted trace) from a GFL neuron after 3 days in culture. The solid lines are the best fit of a single exponential for the SD tail current (bulb, τ_{SD} = 1.45 ms; soma, τ_{SD} = 1.57 ms). The value of this fit at the time of peak tail current was used to calculate the fraction of FD Ca channels (as a percentage of FD + SD Ca channels) for the alternate analysis paradigm (axonal bulb 16, R_S = 0.78 MΩ and C_{in} = 18.6 pF; axotomized soma 11, R_S = 0.42 MΩ and C_{in} = 57.3 pF). (*B*) Records from *A* following subtraction of the SD component (bulb, τ_{FD} = 114 μs; soma, τ_{FD} = 187 μs). (*C*) G_{FD}–*V* relation for the cells in *A*. G_{FD} values are shown fit with single Boltzmann functions of the form $G_{max}/1 + \exp[(V_m - V_{1/2})/k]$, where G_{max} is the maximal conductance density, $V_{1/2}$ is the half-activation voltage, and k is the steepness factor for the fit [bulb (solid circles), G_{max} = 1.23 nS/pF, $V_{1/2}$ = +0.5 mV, and k = 7.4 mV; soma (open circles), G_{max} = 0.21 nS/pF, $V_{1/2}$ = +0.1 mV, and k = 9.0 mV].

ω-Aga IVA Block of FD Ca Channels. Rapidity of activation/deactivation and lack of inactivation of FD Ca channels are all similar to properties of transmitter release-related Ca channels at the squid giant synapse (5), suggesting that FD Ca channels might also be sensitive to toxins isolated from funnel web spider venom that block Ca channels linked to neurotransmitter release and synaptic transmission (9, 15, 20–23).

Fig. 3*A* shows I_{Ca} in a GFL neuron cell body at 0 mV before (solid circles) and after addition of 500 nM ω-Aga IVA (open circles). Neither activation nor inactivation kinetics are altered in the presence of ω-Aga IVA, and similar blocking properties were observed in both somatic and bulbar domains. Examination of the tail currents in Fig. 3*A* shows that only FD Ca channels are blocked by the toxin, because the amplitude of the SD tail in ω-Aga IVA is indistinguishable from the control. FD Ca channel block appears to be independent of the test pulse voltage (−20 to +20 mV range) and holding potential (−120 to −60 mV range; data not illustrated). Fig. 3*B* shows the dose dependence of ω-Aga IVA block, plotting the ratio (±SEM) of peak I_{Ca} in the presence (I) and absence (I_{max}) of toxin (diamonds). The best fit for these data (solid curve) yields a Hill coefficient of 1.4 and an IC_{50} of 420 nM, assuming that all I_{Ca} can be blocked. This is an oversimplification, however, because ω-Aga IVA-insensitive SD Ca channels contribute to peak I_{Ca} at 0 mV and thereby lead to an underestimate of the degree of FD Ca channel block by ω-Aga IVA. Circles in Fig. 3*B* plot the mean I/I_{max} values for the same cells after subtraction of the SD contribution to I_{Ca} determined by tail current analysis. For these data, the Hill coefficient remains 1.4, but the estimated IC_{50} decreases to 242 nM (dashed curve).

ω-Aga IVA block is relieved by depolarizing pulses in rat cerebellar Purkinje cells (ten 60-ms pulses to +130 mV at 1-s intervals; ref. 30), and block of squid FD Ca channels is similarly relieved by depolarization. In Fig. 3*C*, two 25-ms test pulses to 0 mV (P1 and P2, *Inset*) were separated by a variable duration (Δt) step to +80 mV. I_{Ca} during periods P1 and P2 for Δt = 2.5, 25, 100, and 500 ms are shown in the presence of 500 nM ω-Aga IVA, and for comparison the control I_{Ca} (no ω-Aga IVA) during P1 is illustrated. As Δt increases, the amplitude of I_{Ca} during P2 progressively increases, and 100% of control I_{Ca} is recovered with Δt = 500 ms.

Subcellular Localization of FD Ca Channels. Cultured GFL neurons have been previously utilized to demonstrate appropriate targeting of giant axon-type Na channels to growing axonal bulbs (11, 14). Na channel density in axonal bulbs is initially very small but increases dramatically over time in culture. These results contrast markedly with our observations for FD Ca channels (Fig. 4). FD Ca channels are present in "acutely isolated" axonal bulbs on day 0 *in vitro* (recordings performed <6 h after dissection), and G_{FD} at this time is higher in axonal bulbs (solid bars) than in somata (hatched bars). As axonal bulbs grow larger in culture, G_{FD} does not change significantly in either domain during the time when bulbar G_{Na} increases to a high level (open circles).

Although G_{FD} values for both bulbs and somata are relatively constant over 9 days *in vitro*, the amount of FD Ca conductance in a typical bulb (g_{FD} bulb, Table 1) increases considerably during this time, and total cellular FD Ca conductance measured in individual neurons [total g_{FD} = g_{FD} (bulb) + g_{FD} (soma)] increases ≈2-fold. This increase in total g_{FD} indicates that additional channels are synthesized and expressed at the plasma membrane in culture, and the conjugate increases in bulbar g_{FD} and in the percentage of FD Ca channels in axonal bulbs (percent g_{FD} bulb) implies that the bulk of these newly synthesized FD Ca channels are specifically incorporated into the axonal bulb.

DISCUSSION

We have analyzed the properties and spatial distribution of FD Ca channels in somatic and extrasomatic domains of squid GFL neurons. These channels are of interest because they possess similar properties to presynaptic Ca channels found at the squid giant synapse (5) and presynaptic membranes of other neurons (16, 17).

To determine G_{FD}, we have assumed that FD and SD Ca currents arise from independent channel populations in GFL neurons (see ref. 25), rather than from a single population with a nonexponential deactivation time course (26–28). Although neither our data nor those of others (12, 13) have revealed a clear set of properties for SD channels, conclusions discussed

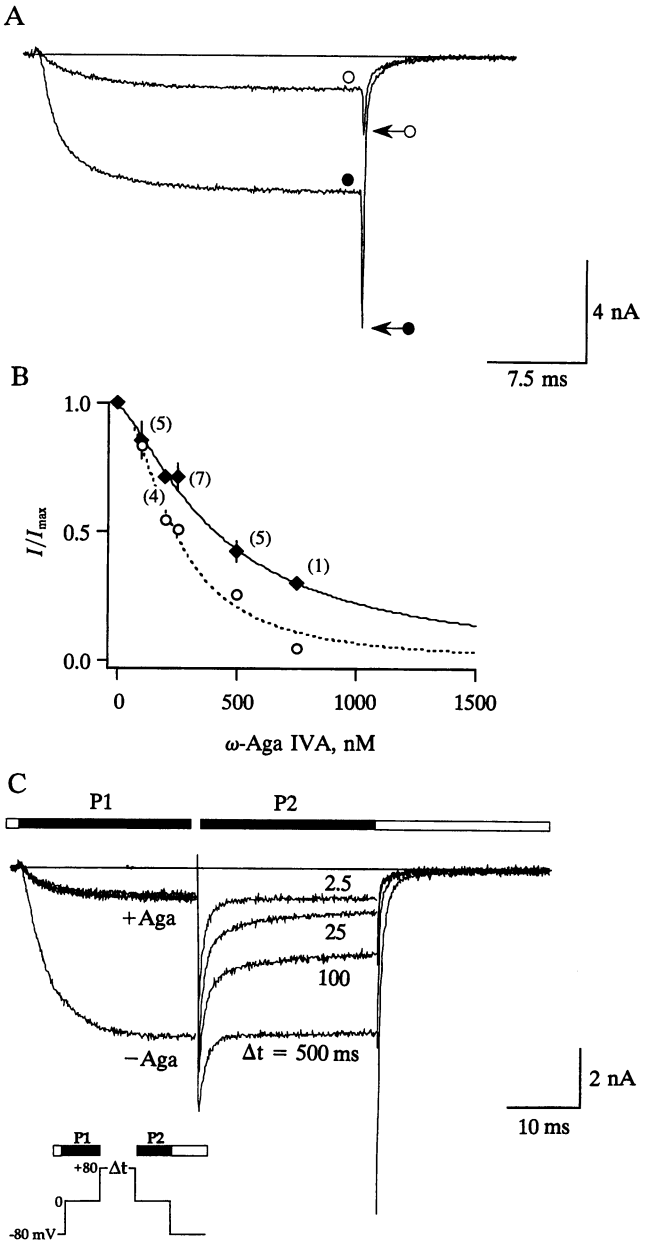

FIG. 3. ω-Aga IVA block of FD Ca channels. (*A*) Block of whole-cell I_{Ca} at 0 mV by ω-Aga IVA in an axonless GFL neuron (solid circle, control; open circle, 500 nM ω-Aga IVA) (cell 13sep94a, R_S = 0.28 MΩ and C_{in} = 144 pF). (*B*) Dose dependence of I_{Ca} block by ω-Aga IVA. I/I_{max} (diamonds) was determined by dividing peak inward current after step depolarization to 0 mV in the presence of ω-Aga IVA by the control value. Small numbers in parentheses indicate the number of observations. The data are shown fit with the Hill equation, $y = x^n/(x^n + q^n)$, where variables n and q represent the Hill coefficient and concentration for 50% inhibition, respectively. The dashed line shows the Hill equation fit for mean I/I_{max} values after subtraction of the SD Ca channel component of I_{Ca} for each cell (circles). The Hill coefficient remains 1.4, but the estimated IC_{50} decreases to 224 nM. (*C*) Depolarization induces the relief of ω-Aga IVA block (pulse pattern shown in *Inset*). Two pulses to 0 mV for 25 ms (P1 and P2) were separated by a step of variable duration to +80 mV (Δt). Four traces are shown for Δt = 2.5, 25, 100, and 500 ms in the presence of 500 nM ω-Aga IVA. Control I_{Ca} (−Aga) during period P1 is shown for comparison, demonstrating that ω-Aga IVA block is completely relieved during P2 for Δt = 500 ms (cell 13sep94a).

here are not contingent on the exact identity of the SD channels.

Properties of FD Ca channels in axonal bulbs and in somata are very similar; however, results shown in Fig. 2*B* demonstrate

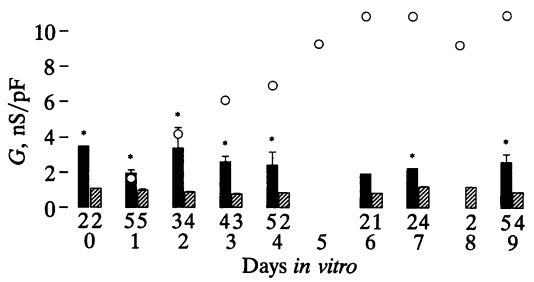

FIG. 4. Subcellular localization of Na and FD Ca channels in GFL neuronal membranes. Maximum FD Ca channel conductance density (G_{FD}) in axonal bulbs (solid bars) and axotomized soma (hatched bars) expressed as a function of culture time. G_{FD} values were estimated from FD tail current amplitudes. Small numbers below each bar correspond to the number of observations. Significance was judged by t test. *, $P < 0.05$ for bulbs vs. somata. Mean conductance density of prepulse-sensitive sodium channels (G_{Na}) in axonal bulbs is shown for comparison (open circles, from ref. 11).

that the rate of FD Ca channel deactivation is measurably faster in axonal bulbs than in axotomized somata. This small difference can be observed consistently at all times in culture including on day 0, and we do not regard this difference as indicative of different FD Ca channel types in the two domains. A more dramatic example of spatially distinct properties has been demonstrated for Ca channel inactivation in the cell body of molluscan giant neurons (29).

Toxins isolated from funnel-web spider venom act in several preparations to block Ca channels that have kinetic characteristics similar to those displayed by FD Ca channels in GFL neurons (9, 15, 30). Ca channel sensitivity to block by a polyamine (funnel-web spider toxin or FTX) or peptide (ω-Aga IVA) component of this venom provides the pharmacological definition for the family of P-type Ca channels (15). Block of P-type Ca channels inhibits the presynaptic Ca influx required for neurotransmitter release from brain synaptosomes (23), at central synapses (22) and at neuromuscular junctions (20, 31). Other pharmacologically defined Ca channel types also exist in presynaptic nerve terminal preparations, and participation of these multiple channel types in transmitter release remains unclear (16, 32, 33). In the presynaptic element of the squid giant synapse, a single population of FTX-sensitive Ca channels appears to be responsible for synaptic transmission (5, 9, 15).

Our results show that GFL Ca channels display strong biophysical similarities to squid presynaptic Ca channels as well as vertebrate P-type Ca channels; however, GFL FD Ca channels deviate from the expected pharmacological profile for P-type Ca channels. ω-Aga IVA blocks without affecting activation, inactivation, or deactivation kinetics just as in rat central neurons (30, 34), yet our estimated K_d for GFL FD Ca channels of 240–420 nM is considerably higher than the value obtained in rat cerebellar Purkinje cells ($K_d \approx 1$ nM; ref. 24). Lower ω-Aga IVA sensitivity is a characteristic of the vertebrate Q-type Ca channel (34), but in the absence of specific molecular information, precise identification of squid FD Ca channels as either P- or Q-type may not be appropriate (see ref. 24). Low sensitivity to ω-Aga IVA block in the 10^{-7} M range is also observed for neuromuscular transmission in crayfish (20) and crab (21), and classification of Ca channels in phylogenetically distant organisms using criteria based on vertebrate pharmacology is not likely to be simple.

Even within the vertebrates, distinction between these channel types may be blurred. Differences in P- and Q-type properties, including ω-Aga IVA sensitivity, need not even reflect primary structural differences in these channels but could result from differential posttranslational modifications or any number of possibilities. For example, biophysical properties (but not ω-Aga

Table 1. Comparison of amount and density of FD Ca channel conductance in axonal bulbs and axotomized somata over time in culture

Parameter	Culture time (days)		
	1 day	7 days	9 days
Bulb G_{FD}, nS/pF	1.51 ± 0.24	1.41 ± 0.31	2.38 ± 0.31
Soma G_{FD}, nS/pF	0.34 ± 0.12	0.58 ± 0.04	0.31 ± 0.06
g_{FD} (bulb), nS	27.4 ± 5.6	90.7 ± 30.0	152.4 ± 64.3
g_{FD} (soma), nS	63.3 ± 29.5	58.6 ± 5.2	26.0 ± 5.5
Total g_{FD}, nS	90.7 ± 34.9	149.3 ± 34.7	178.4 ± 64.6
% g_{FD} (bulb)	41.8 ± 10.2	56.5 ± 6.4	77.4 ± 9.9
Bulb surface area, μm^2	22.7 ± 4.2	47.0 ± 14.0	64.2 ± 17.7

Each data set was obtained from cells where recording from both bulb and somata was achieved ($n = 4$ for each case). g_{FD} in all cases is estimated from I_{FD} derived from peak I_{Ca}. G_{FD} was determined by dividing this value by the total input capacitance. g_{FD} values from individual bulb–soma pairs were summed to obtain the total g_{FD}, and these values were used to compute the mean. Similarly, the percentage of g_{FD} in the bulb (% g_{FD} bulb) represents the mean of the values computed for individual GFL neurons. Surface area was determined from input capacity by assuming 1 $\mu F = 1\ cm^2$.

IVA sensitivity) of rat brain α_{1A} Ca channel subunits expressed in *Xenopus* oocytes are greatly altered by coexpression with several β subunits (24). Similarly, significant differences in sensitivity to agitoxin 2 (a polypeptide toxin from scorpion venom) are observed for the same Kv1-type potassium channel (Shaker Δ6-46) α subunits expressed in oocytes ($K_d < 1$ nM; ref. 34) versus Sf9 cells ($K_d > 100$ nM; unpublished observations).

Despite the lower affinity, a distinguishing feature of ω-Aga IVA block is shared between squid and P-type Ca channels identified in rat neurons (30). In both cases, relief of toxin block is produced by strong depolarization, which has been presumed to induce the unbinding of ω-Aga IVA from the external surface of the channel by electrostatic repulsion (30). The strength of depolarization required to achieve full relief of block of squid FD Ca channels is smaller than in Purkinje cells and probably results from the lower affinity of ω-Aga IVA for the GFL Ca channel.

Cultured GFL neurons maintain FD Ca channels at a higher density in growing axonal bulbs than in the supporting cell bodies, and we propose that GFL FD Ca channels, like Na channels (11), are normally targeted for expression in extrasomatic domains of the neuron. For Na channels, this domain is the giant axon, but this is not likely to be true for FD Ca channels. Voltage-dependent I_{Ca} density recorded from giant axons is much smaller (≈3 pA/pF in 80 mM Ca; ref. 18) than in axonal bulbs (up to 100 pA/pF in 50 mM Ca), and kinetic properties of these two types of I_{Ca} are different. FD Ca channels incorporated into axonal bulbs *in vitro* may represent those channels that are transported along the giant axon to the extensive arborization of motor terminals, but the evidence presented here to support this claim is admittedly circumstantial. Similarly, rigorous proof of preferential expression of FD Ca channels in growing axonal bulbs would require knowledge of channel turnover rate in both neuronal domains, but pertinent data are not available.

Thus, the biophysical properties and qualitative features of ω-Aga IVA sensitivity demonstrate similarity between GFL neuron FD Ca channels and the Ca channels that subserve synaptic transmission in squid. Although we cannot at present firmly associate FD Ca channels in GFL neurons with transmitter release at the neuromuscular junction, the spatial pattern of Ca channel expression in these neurons *in vitro* is consistent with this possibility. Indeed, preliminary experiments indicate that micromolar concentrations of ω-Aga IVA reversibly inhibit squid mantle muscle contraction evoked by electrical stimulation of the stellate ganglion. Complete characterization of the anatomical and physiological properties of this motor unit requires further investigation, but the cultured GFL neuron system may provide a valuable system for physiological, biochemical, and cell biological studies of these Ca channels.

We thank Drs. Nicholas Saccomano (Pfizer) and Richard W. Tsien for gifts of ω-Aga IVA and Drs. M. Bruce MacIver and Richard W. Tsien for helpful suggestions on an earlier version of the manuscript. Recombinant baculovirus carrying Shaker Δ6-46 was kindly provided by Dr. Min Li, and agitoxin 2 was a gift from Dr. Roderick MacKinnon. This work was supported by grants from the National Institutes of Health and the Ford Foundation.

1. Hille, B. (1992) *Ionic Channels of Excitable Membranes* (Sinauer, Sunderland, MA), 2nd Ed.
2. Hagiwara, S. & Byerly, L. (1981) *Annu. Rev. Neurosci.* **4,** 69–125.
3. Hess, P. (1990) *Annu. Rev. Neurosci.* **13,** 337–356.
4. Augustine, G. J., Charlton, M. P. & Smith, S. J. (1987) *Annu. Rev. Neurosci.* **10,** 533–593.
5. Llinás, R., Steinberg, I. Z. & Walton, K. (1981) *Biophys. J.* **33,** 289–322.
6. Robitaille, R., Adler, E. M. & Charlton, M. P. (1990) *Neuron* **5,** 773–779.
7. Smith, S. J., Buchanan, J., Osses, L. R., Charlton, M. P. & Augustine, G. J. (1993) *J. Physiol. (London)* **472,** 573–593.
8. Charlton, M. P. & Augustine, G. J. (1990) *Brain Res.* **525,** 133–139.
9. Llinás, R., Sugimori, M., Lin, J.-W. & Cherksey, B. (1989) *Proc. Natl. Acad. Sci. USA* **86,** 1689–1693.
10. Young, J. Z. (1939) *Philos. Trans. R. Soc. London (Biol.)* **229,** 465–505.
11. Gilly, W. F., Lucero, M. T. & Horrigan, F. T. (1990) *Neuron* **5,** 663–674.
12. Lláno, I. & Bookman, R. J. (1986) *J. Gen. Physiol.* **88,** 543–569.
13. Chow, R. H. (1991) *J. Gen. Physiol.* **98,** 751–770.
14. Gilly, W. F. & Brismar, T. (1989) *J. Neurosci.* **9,** 1362–1374.
15. Llinás, R., Sugimori, M., Hillman, D. E. & Cherksey, B. (1992) *Trends Neurosci.* **15,** 351–355.
16. Stanley, E. F. & Goping, G. (1991) *J. Neurosci.* **11,** 985–993.
17. Yazejian, B., Meriney, S. D. & Grinnell, A. D. (1993) *Soc. Neurosci. Abstr.* **19,** 255.4.
18. DiPolo, R., Caputo, C. & Bezanilla, F. (1983) *Proc. Natl. Acad. Sci. USA* **80,** 1743–1745.
19. Jewell, B. R. & Ruegg, J. C. (1966) *Proc. R. Soc. London* **164,** 428–459.
20. Araque, A., Clarac, F. & Buño, W. (1994) *Proc. Natl. Acad. Sci. USA* **91,** 4224–4228.
21. Hurley, L. M. & Graubard, K. (1995) *Biophys. J.* **68,** 208 (abstr.).
22. Regehr, W. G. & Mintz, I. M. (1994) *Neuron* **12,** 605–613.
23. Turner, T. J., Adams, M. E. & Dunlap, K. (1992) *Science* **258,** 310–313.
24. Stea, A., Tomlinson, W. J., Soong, T. W., Bourinet, E., Dubel, S. J., Vincent, S. R. & Snutch, T. P. (1994) *Proc. Natl. Acad. Sci. USA* **91,** 10576–10580.
25. Matteson, D. R. & Armstrong, C. M. (1986) *J. Gen. Physiol.* **87,** 161–182.
26. Brown, A. M., Tsuda, Y. & Wilson, D. L. (1983) *J. Physiol. (London)* **344,** 549–583.
27. Byerly, L., Chase, P. B. & Stimers, J. R. (1984) *J. Physiol. (London)* **348,** 187–207.
28. Taylor, W. R. (1988) *J. Physiol. (London)* **407,** 405–432.
29. Thompson, S. & Coombs, J. (1988) *J. Neurosci.* **8,** 1929–1939.
30. Mintz, I. M., Adams, M. E. & Bean, B. P. (1992) *Neuron* **9,** 85–95.
31. Uchitel, O. D., Protti, D. A., Sanchez, V., Cherksey, B., Sugimori, M. & Llinás, R. (1992) *Proc. Natl. Acad. Sci. USA* **89,** 3330–3333.
32. Heidelberger, R. & Matthews, G. (1992) *J. Physiol. (London)* **447,** 235–256.
33. Lemos, J. R. & Nowycky, M. C. (1989) *Neuron* **2,** 1419–1426.
34. Randall, A. & Tsien, R. W. (1995) *J. Neurosci.* **15,** 2995–3012.
35. Garcia, M. L., Garcia-Calvo, M., Hidalgo, P., Lee, A. & MacKinnon, R. (1994) *Biochemistry* **33,** 6834–6839.